# Interaction of CD 3 CN and Pyridine with the Ti(IV) Centers of TS1 Catalysts: a Spectroscopic and Computational Study

**ARTICLE** *in* LANGMUIR · MARCH 2003

Impact Factor: 4.46 · DOI: 10.1021/la0262194



**5 AUTHORS**, INCLUDING:

Carlo Lamberti
Università degli Studi di Torino
**382** PUBLICATIONS **13,162** CITATIONS
SEE PROFILE

A. Zecchina
Università degli Studi di Torino
**560** PUBLICATIONS **20,148** CITATIONS
SEE PROFILE

# Interaction of $CD_3CN$ and Pyridine with the Ti(IV) Centers of TS-1 Catalysts: a Spectroscopic and Computational Study

Francesca Bonino,[†] Alessandro Damin,[†] Silvia Bordiga,*[,‡] Carlo Lamberti,[‡] and Adriano Zecchina[†]

*Department of Inorganic, Physical, and Material Chemistry, University of Turin, Via P. Giuria 7, 10125 Torino, Italy and INSTM UdR Torino Università, Torino, Italy*

*Received July 10, 2002. In Final Form: December 4, 2002*

In this paper, we describe the interaction of $CD_3CN$ and pyridine (used as probes of Lewis acid centers) with TS-1 catalyst. Interaction of $CD_3CN$ and pyridine with Ti(IV) centers leads to surface adducts characterized by well-defined IR spectra which can be distinguished from those ascribed to interaction with internal hydroxyl groups, which are the most abundant acidic species present in TS-1. In both cases, spectroscopic features were observed which are characteristic of TS-1 and completely absent in pure siliceous silicalite-1. This IR study has demonstrated that Ti(IV) centers embedded in the MFI framework have a Lewis acidity strength comparable of that of Ti(IV) sites at the surface of $TiO_2$. The spectroscopic results have been compared with computational data obtained on cluster models on the basis of the ONIOM approach.

## 1. Introduction

Titanium silicalite-1 (TS-1) is a synthetic zeolite in which a few Ti atoms substitute tetrahedral Si atoms in a purely siliceous framework with the MFI structure.[1,2] It is an active and selective catalyst in several low-temperature oxidation reactions with aqueous $H_2O_2$ as the oxidant agent.[3−7] For this reason, it has been one of the most studied materials in heterogeneous catalysis in the last years.[3−12] The difficulty in the characterization of Ti(IV) Lewis centers in TS-1 is two-fold: (i) the high dilution of Ti(IV) (less than 3 wt % in $TiO_2$[8]) and (ii) the presence of framework defects (Si vacancies) generating internal hydroxyl groups (silanols as well as titanols acting as weak Brønsted sites).[13,14] As a consequence, it is very difficult to distinguish the spectroscopic features related to Ti(IV) species from those due to hydroxyl groups. Main attention has been devoted, in the past, to the study of TS-1 reactivity toward $H_2O$ and $NH_3$. It was concluded that it is difficult to isolate the direct interaction of Ti(IV) with $H_2O$ and $NH_3$ from that ascribed to the interaction with silanols and titanols.[14]

In the present paper, we want to discuss the experimental evidences for the presence of Lewis acidic centers associated with Ti(IV) in TS-1 by studying the vibrational properties of $CD_3CN$ and pyridine adsorbed on TS-1. The choice of these two molecules seems to be more appropriate than water and ammonia for this specific aim, since the spectroscopic features of $CD_3CN$ and pyridine are different when adsorbed on Lewis or on Brønsted sites. To confirm our assignments, the vibrational features observed on TS-1 will be compared with those obtained by adsorbing $CD_3CN$ and pyridine on a Ti free silicalite-1 matrix used as blank material hosting only Brønsted sites. Finally, the definitive validation will come from the comparison between experimental and computed frequencies obtained on a cluster model.

## 2. Experimental Section

**2.1. Samples and Experimental Methods.** Both TS-1 and silicalite-1 samples were synthesized in the PolimeriEuropa laboratories following a procedure described in the original patent.[1] The Ti-content, expressed in $TiO_2$ wt %, is 3.0. The complete insertion of Ti atoms in the MFI framework has been proved by verifying that the amount of Ti determined by chemical analysis is the same required to cause the expansion of the cell volumes measured by Rietveld refinement of powder XRD data, see refs 8 and 15 for more details.

The IR spectra (resolution: 2 $cm^{-1}$) were measured on a Bruker IFS 66 FTIR spectrometer equipped with a HgCdTe cryodetector. Samples have been studied in transmission mode as thin self-supported wafers. $CD_3CN$ and pyridine were dosed on the samples previously activated in a dynamical vacuum of $10^{-4}$ Torr, from the gas phase through a vacuum manifold directly connected with the cell. Silicalite-1 samples were outgassed under vacuum

* To whom correspondence should be addressed. Tel.: +39011-6707858. Fax: +39011-6707855. E-mail: silvia.bordiga@unito.it.
† University of Turin.
‡ INFM UdR Torino Università.

(1) Taramasso, M.; Perego, G.; Notari, B. U.S. Patent 4410501, 1983.
(2) Meier, W. M.; Olson, D. H.; Baerlocher, Ch. *Atlas of Zeolite Structure Types*; Elsevier: London, 1996.
(3) Clerici, G. M.; Bellussi, G.; Romano, U. *J. Catal.* **1991**, *129*, 159.
(4) Bellussi, G.; Carati, A.; Clerici, G. M.; Maddinelli, G.; Millini, R. *J. Catal.* **1992**, *133*, 220.
(5) Notari, B. *Adv. Catal.* **1996**, *41*, 253, and references therein.
(6) Mantegazza, M. A.; Petrini, G.; Spanò, G.; Bagatin, R.; Rivetti, F. *J. Mol. Catal. A* **1999**, *146*, 223.
(7) Bordiga, S.; Damin, A.; Bonino, F.; Ricchiardi, G.; Lamberti, C.; Zecchina, A. *Angew. Chem., Int. Ed.* **2002**, *41*, 4734.
(8) Millini, R.; Previdi Massara, E.; Perego, G.; Bellussi, G. *J. Catal.* **1992**, *137*, 497.
(9) Vayssilov, G. N. *Catal. Rev. Sci. Eng.* **1997**, *39*, 209.
(10) Tozzola, G.; Mantegazza, M. A.; Ranghino, G.; Petrini, G.; Bordiga, S.; Ricchiardi, G.; Lamberti, C.; Zulian, R.; Zecchina, A. *J. Catal.* **1998**, *179*, 64.
(11) Ricchiardi, G.; de Man, A.; Sauer, J. *Phys. Chem. Chem. Phys.* **2000**, *2*, 2195.
(12) Sinclair, P. E.; Sankar, G.; Catlow, C. R. A.; Thomas, J. M.; Maschmeyer, T. *J. Phys. Chem. B* **1997**, *101*, 4232.
(13) Bolis, V.; Bordiga, S.; Lamberti, C.; Zecchina, A.; Petrini, G.; Rivetti, F.; Spanò, G. *Langmuir* **1999**, *15*, 5753.
(14) Bordiga, S.; Damin, A.; Bonino, F.; Zecchina, A.; Spanò, G.; Rivetti, F.; Bolis, V.; Lamberti, C. *J. Phys. Chem. B* **2002**, *106*, 9892, and references therein.
(15) (a) Lamberti, C.; Bordiga, S.; Zecchina, A.; Carati, A.; Fitch, A. N.; Artioli, G.; Petrini, G.; Salvalaggio, M.; Marra, G. L. *J. Catal.* **1999**, *183*, 222. (b) Lamberti, C.; Bordiga, S.; Zecchina, A.; Artioli, G.; Marra, G. L.; Spanò, G. *J. Am. Chem. Soc.* **2001**, *123*, 2204.

10.1021/la0262194 CCC: $25.00 
Published on Web 01/30/2003

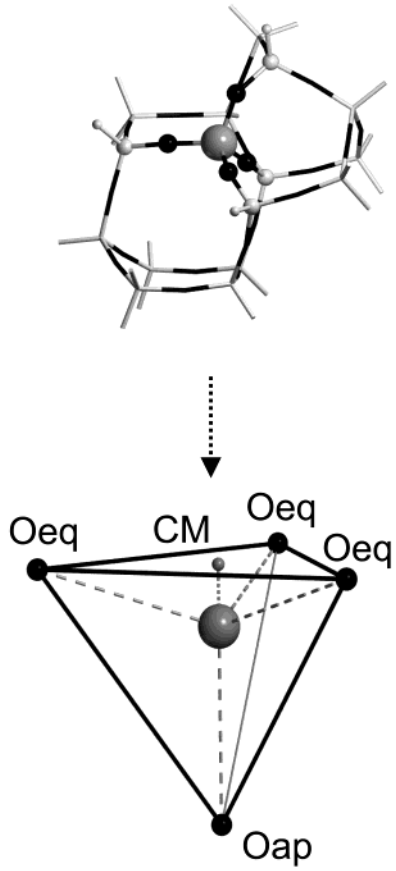


**Figure 1.** MFI_T16 ($TiSi_{15}O_{22}H_{20}$) bare cluster model (top) and schematic representation of the Ti(IV) first shell ($TiO_4$ unit, bottom). For the MFI_T16 cluster, the sticks and balls vs the sticks notation discriminates the model zone (where the link H atoms are omitted for clarity) from the complementary part of the cluster treated at a low level only. Gray, black, and white colors define Ti, O, and (Si or H) atoms. In the bottom picture, the dotted arrow represents the absorption direction of a ligand molecule (L = $CH_3CN$ or $C_5H_5N$), which breaks the symmetry of the four first neighbor oxygen atoms into three equatorial (Oeq) and one apical (Oap). The small gray sphere shows the center of mass of the three Oeq atoms (labeled as CM in the text).

at 823 K, while TS-1 samples were pretreated at 673 K. These slightly different temperatures have been adopted because it has been experimentally verified that they lead to a comparable "free" silanol population.[16]

In the IR experiments, $CD_3CN$ has been used instead of $CH_3CN$ to avoid the well-known spectroscopic complication due to Fermi resonance between the $\bar{\nu}$(CN) vibration and the combination mode $\delta(CH_3) + \bar{\nu}(CC)$.[17,18]

**2.2. Models and Computational Details.** In this work, a cluster model (MFI_T16, see top part of Figure 1) is used to simulate the Ti site in TS-1 and to study its interaction with $CH_3CN$ and pyridine molecules. This nomenclature comes from ref 19, which makes a systematic methodological comparison among $TiO_4$ unit embedded in different hosting clusters of increasing size: $Ti(OH)_4$ (model T1), $Ti(SiOH_3)_4$ (model T5), $TiSi_6O_8H_{12}$ (model T7), CHA_T8, $TiSi_{13}O_{19}H_{18}$ (model MFI_T14), $TiSi_{14}O_{20}H_{20}$ (model MFI_T15), MFI_T16, and $TiSi_{17}O_{26}H_{20}$ (model MFI_T18).

To limit the computational demand in our calculations, the cluster/embedded cluster ONIOM[20] scheme, on the basis of the integration of molecular orbital at different levels of theory,[20b] was adopted with the same scheme employed in refs 14, 19, and 21. The total energy of the ONIOM system, $E$(ONIOM), is obtained from three distinct self-consistent field energy calculations which are combined according to $E(\text{ONIOM}) = E_{\text{High}}(\text{model zone}) + [E_{\text{Low}}(\text{whole cluster}) - E_{\text{Low}}(\text{model zone})]$, being (i) $E_{\text{Low}}$(whole cluster) the energy of the whole cluster calculated at the low level of theory (RHF/3-21G(H,N,C,Si,O), 3-21G*(Ti)); (ii) $E_{\text{Low}}$(model zone) the energy of the model zone computed at the low level of theory (RHF/3-21G(H,C,N,Si,O), 3-21G*(Ti)); (iii) $E_{\text{High}}$(model zone) the energy of the model zone computed at the high level of theory at (B3-LYP/ 6-311+G(d,p)(H,C,N,Si,O), *ppp*(Ti)) high (H) level. Note that *ppp* represents the basis-set employed for the Ti atom which is composed of effective small-core pseudopotentials[22] + LANL2DZ[22] + Ahlrichs TZV "p" polarization function.[23] In cluster MFI_T16, the model zone (stick and balls in Figure 1) corresponds to the T5 model (brutto formula $Ti(SiOH_3)_4$) employed in refs 14, 19, and 21. During the optimization cycles, all atomic positions were free to relax without any artificial constraints imposed on the model zone except for those induced by the whole cluster itself. This role is played by the link atoms which transfer mechanical constraints from the whole cluster to the model zone. In fact, link atoms are forced to stay along the Si−O directions (where Si is the last atom of the model zone and O is the first atom of the zone treated only at lower level).

The insertion of the $Ti(SiOH_3)_4$ unit into the MFI_T16 cluster (Figure 1a) causes a deformation of the original perfect tetrahedral moiety: this process destabilizes the structure which becomes more reactive toward the adsorption of ligands.[14,19,21] In the presence of a ligand, the Ti(IV) center undergoes a further distortion. As a consequence, the four oxygen atoms are no more equivalent and must be divided into three equatorial atoms and one apical atom (Oeq and Oap in the bottom part of Figure 1). The plane perpendicular to the adsorption direction is defined by the three Oeq, Oap lying on the opposite side with respect to the adsorbed molecule. So the 6 O−Ti−O angles of the $TiO_4$ unit (109.5° in perfect $T_d$ symmetry) are no more equivalent upon adsorption: the two triplets Oeq−Ti−Oeq and Oeq−Ti−Oap angles are labeled $\alpha$ and $\beta$, respectively. CM defines the center of mass of the three Oeq atoms (Figure 1).[24] The a posteriori method proposed by Lendvay and Mayer[25] has been used to estimate the basis set superposition error (BSSE). From the computed binding energies (BE), the BSSE corrected binding energies ($BE^c$) are obtained as $BE^c = BE - BSSE$.

## 3. Experimental Results

**3.1 Reactivity of Hydroxyl Groups.** TS-1 and the parent Ti-free Silicalite-1, synthesized following patent,[1] are rather defective materials, showing a high density of internal hydroxylated cavities (nests).[13,14,26,27] The presence of an abundant quantity of SiOH (and possibly TiOH) groups, either isolated or mutually interacting via H-bond, generally obscures any direct evidence of Ti(IV) interaction with probe molecules. The interaction of these hydroxyls

(16) Bordiga, S.; Ugliengo, P.; Damin, A.; Lamberti, C.; Spoto, G.; Spanò, G.; Dalloro, L.; Buzzoni, R.; Rivetti, F.; Zecchina, A. *Top. Catal.* **2001**, *15*, 43.
(17) Venkateswarlu, P. *J. Chem. Phys.* **1951**, *19*, 293.
(18) Angell, C. L.; Howell, M. V. *J. Chem. Phys.* **1969**, *73*, 2551.
(19) Damin, A.; Bordiga, S.; Zecchina, A.; Lamberti, C. *J. Chem. Phys.* **2002**, *117*, 226.
(20) (a) Maseras, F.; Morokuma, K. *J. Comput. Chem.* **1995**, *10*, 1170. (b) Humbel, S.; Sieber, S.; Morokuma, K. *J. Chem. Phys.* **1996**, *105*, 1959. (c) Dapprich, S.; Komaromi, I.; Byun, K. S.; Morokuma, K.; Frisch, M. J. *J. Mol. Struct. THEOCHEM* **1999**, *461*, 1.
(21) Damin, A.; Bonino, F.; Ricchiardi, G.; Bordiga, S.; Zecchina, A.; Lamberti, C. *J. Phys. Chem. B* **2002**, *106*, 7524.
(22) Hay, P. J.; Wadt, W. R. *J. Chem. Phys.* **1985**, *82*, 299.
(23) Schaefer, A.; Huber, C.; Ahlrichs, R. *J. Chem. Phys.* **1994**, *100*, 5829.
(24) The Ti−CM distance moves from 0.334*Ti−O in $T_d$ symmetry (where 0.334 = cos(180−109.5°)) to zero in a perfect bipyramidal symmetry (where the Ti atom lies in the plane defined by the three Oeq atoms). As a consequence, the Ti−CM distance gives a direct measure of the symmetry distortion undergone by the TiO4 moiety upon insertion in a portion of the zeolite framework (model MFI_T16) and upon adsorption of a ligand molecule.
(25) Lendvay, G.; Mayer, I. *Chem. Phys. Lett.* **1998**, *297*, 365.
(26) (a) Bordiga, S.; Roggero, I.; Ugliengo, P.; Zecchina, A.; Bolis, V.; Artioli, G.; Buzzoni, R.; Marra, G. L.; Rivetti, F.; Spanò, G.; Lamberti, C. *J. Chem. Soc., Dalton Trans.* **2000**, 3921. (b) Artioli, G.; Lamberti, C.; Marra, G. L. *Acta Cryst. B* **2000**, *56*, 2.
(27) Bolis, V.; Busco, C.; Bordiga, S.; Ugliengo, P.; Lamberti, C.; Zecchina, A. *Appl. Surf. Sci.* **2002**, *21*, 67.

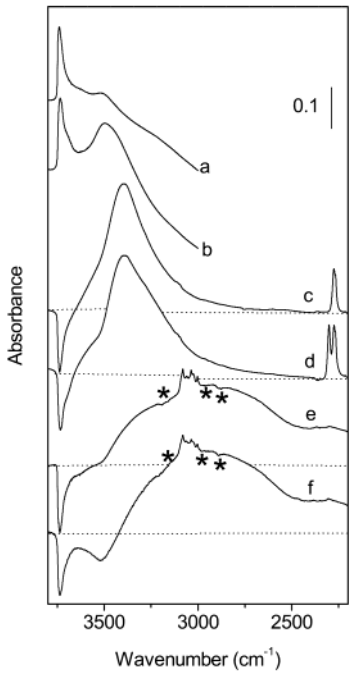


**Figure 2.** From top to bottom: silicalite-1 sample activated at 823 K (a); TS-1 sample activated at 673 K (b); background-subtracted spectrum of silicalite-1 sample upon $CD_3CN$ interaction (c); background-subtracted spectrum of TS-1 sample upon $CD_3CN$ interaction (d); background-subtracted spectrum of silicalite-1 sample upon pyridine interaction (e); background-subtracted spectrum of TS-1 sample upon pyridine interaction (f).

is the main spectroscopic feature, when adsorbing $H_2O$ and $NH_3$, preventing the observation of the interaction with Ti(IV) as active center.[14] As the situation might be different for $CD_3CN$ and pyridine as probes, we have compared the surface properties of TS-1 and silicalite-1 by applying these two molecules (Figure 2). $CD_3CN$ and pyridine were dosed on TS-1 and silicalite-1 samples characterized by a comparable population of isolated silanols (absorbing in the 3750−3650 $cm^{-1}$ range), as can be seen in spectra a and b, respectively. Both spectra are characterized by a complex absorption centered at about 3735 $cm^{-1}$ with a shoulder at 3690 $cm^{-1}$. The absorption at 3735 $cm^{-1}$, characterized by at least two components at 3742 and 3722 $cm^{-1}$, has already been discussed and attributed to unperturbed external and internal silanols (titanols).[16,26,27] The absorption at 3690 $cm^{-1}$ was attributed to substantially unperturbed SiOH species in terminal position in hydrogen-bonded silanol chains (vide infra). Moving to lower frequency, the broad band centered at 3500 $cm^{-1}$ is due to hydrogen-bonded SiOH (TiOH) groups (grouped into chains) located in the nests.[16,26,27] This component is stronger on the TS-1 sample, as the silicalite-1 one has been outgassed at higher temperature. We will see that, as far as the reactivity of hydroxyl groups toward probe molecules is concerned, the major role is played by free species; consequently, the difference in concentration of hydrogen-bonded species in the TS-1 and silicalite-1 samples has no relevance in the present paper.

Upon $CD_3CN$ dosage on TS-1 and silicalite-1, we observe the total erosion of free hydroxyl groups and a parallel growth of a broad absorption centered at about 3400 $cm^{-1}$ because of the formation of $CD_3CN$....OH adducts (curves c and d). The identical shift of the hydroxyl groups of both matrixes, upon probe dosage, is a further indication that, as far as the Brønsted acidity is concerned, silicalite-1 and TS-1 are indistinguishable.

As the H-bonded species, formed upon interaction, contribute to the IR spectra with a strong and very broad band extending down to 3000 $cm^{-1}$, it is difficult to determine the destiny of the component originally centered at 3500 $cm^{-1}$ (hydroxyl groups mutually interacting in the nests) characteristic of the TS-1 sample activated at 673 K. However, whatever the fate of these species, they are not more perturbed than the isolated ones, because we do not observe the preferential formation of lower frequency bands on TS-1. All these considerations suggest that the reactivity toward $CD_3CN$ of hydroxyl groups of silicalite-1 and TS-1 is equivalent and that silicalite-1 and TS-1 cannot be differentiated on this basis.[28,29] We anticipate that a different conclusion will be obtained through the examination of $\bar{\nu}$(CN) stretching region (vide infra).

Moving now to the discussion of the results obtained upon pyridine interaction, some specific considerations related to pyridine adsorption have to be added. First of all, because of the molecular dimension (quite big with respect to the MFI pore diameter), the IR spectra collected after each dose are time-dependent, because of diffusion effects. This is the reason why, in order to report only equilibrium data, we present the results related to spectra obtained after RT vapor pressure pyridine contact, equilibration, and successive desorption in steps. Second, the filling of the channels and cavities with pyridine is causing not only a perturbation of the IR spectra of pyridine but is also perturbing the spectra of the hosting zeolitic matrix. In fact, upon pyridine dosage, a perturbation of zeolitic skeletal combination modes is observed: bands originally at 2005, 1884, and 1645 $cm^{-1}$ shift to 1986, 1872, and 1637 $cm^{-1}$, respectively (spectral region omitted in the figure). The third observation is that desorption of pyridine at room temperature is a slow process.

The effects of pyridine interaction with isolated hydroxyl groups are very similar to those found in $CD_3CN$, that is, total disappearance of the band centered at 3735 $cm^{-1}$ and parallel formation of a broad band at lower frequency because of the formation of Py···OH adduct. Of course, as pyridine is stronger base than $CD_3CN$, the center of mass of the broad absorption associated with H-bonded species is shifted to lower frequency (3000 vs 3400 $cm^{-1}$) both for silicalite-1 and for TS-1 samples, see Figure 2 curves e and f, respectively.

The spectra in the 3500−2500 region are complex not only because of the superposition of $\bar{\nu}$(CH) stretching modes (bands at 3081, 3036−3028, and 3007−3002 $cm^{-1}$)[30] but also because Fermi resonance effects[31,32] lead to the formation of resonance "windows" in the broad bands because of H-bonded species (indicated by ∗ in the figure). In particular, we note the presence of minima in the 2960−2900 $cm^{-1}$ interval, which can be assigned to Fermi resonance effects of the $\bar{\nu}$(O−H···Py) mode with overtones and combinations of the pyridine ring stretching modes (1480−1425 $cm^{-1}$ range). An equivalent explanation can be given, at least in principle, for the minima observed in the interval 3200−3100 $cm^{-1}$. In this case, the phenomenon is due to resonance of $\bar{\nu}$(O−H···Py) mode with overtones of pyridine ring modes in the 1600−1570 $cm^{-1}$

(28) Armaroli, T.; Milella, F.; Notari, B.; Willey, R. J.; Busca, G. *Top. Catal.* **2001**, *15*, 63.
(29) Armaroli, T.; Bevilacqua, Trombetta, M.; Milella, F.; Gutiérrez Alejandre, A.; Ramírez, J.; Notari, B.; Willey, R. J.; Busca, G. *Appl. Catal.* **2001**, *216*, 59.
(30) Kline, C. H.; Turkevich, J. *J. Chem. Phys.* **1944**, *12*, 300.
(31) Buzzoni, R.; Bordiga, S.; Ricchiardi, G.; Lamberti, C.; Zecchina, A.; Bellussi, G. *Langmuir* **1996**, *12*, 930.
(32) Pazé, C.; Bordiga, S.; Lamberti, C.; Salvalaggio, M.; Zecchina, A.; Bellussi, G. *J. Phys. Chem. B* **1997**, *101*, 4740.

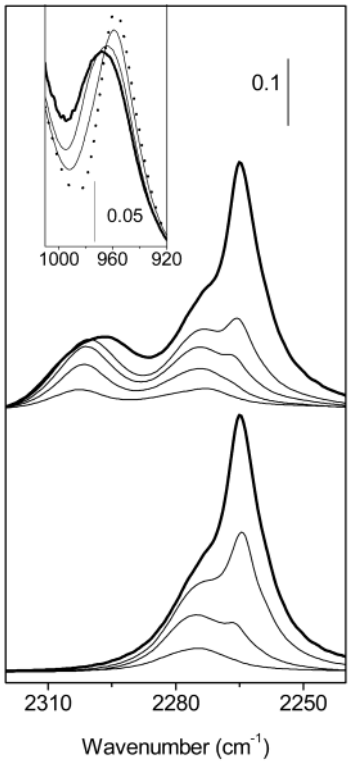


**Figure 3.** Background-subtracted spectra of increasing coverages of $CD_3CN$ on TS-1 (top) and silicalite-1 (bottom): $\bar{\nu}$(CN) region. The spectra obtained at high $CD_3CN$ coverage are reported with the bold line. The inset reports the perturbative effect of $CD_3CN$ on the 960 $cm^{-1}$ band: the pure TS-1 spectrum is reported with a dotted line, while the bold line reports the spectrum obtained at high $CD_3CN$ coverage.

range. Fermi resonance effects between $\bar{\nu}$(O−H···Py) mode and the overtone of the $\delta$(O−H···Py) mode (at about 1150 $cm^{-1}$) is likely responsible of different minima at $\bar{\nu} < 2500$ $cm^{-1}$ occurring on the absorption tail. As a final consideration of the broad band due to OH···Py adducts, we draw the attention to the fact that background subtracted spectra show an apparent absorption extending to a frequency region where the contribution of the tail of $\bar{\nu}$-(O−H···Py) mode should be negligible. This is likely due to the fact that upon pyridine interaction the sample scattering profile changes, thus causing the appearance of anomalous spectra profiles.

On TS-1 sample we clearly observe, upon pyridine interaction, the total disappearance not only of the $\bar{\nu}$(O−H) of the free silanols but also the disappearance of the absorption associated with hydrogen-bonded species in the nests (band centered at 3500 $cm^{-1}$). However, the interaction of pyridine with these species is not associated with a stronger perturbation of the $\bar{\nu}$(O−H); in fact, the spectra of TS-1 and pure silicalite-1 (curves e and f) are totally equivalent in the 3400−2400 $cm^{-1}$ range.

**3.2 The Ti(IV)/$CD_3CN$ Adducts.** Figure 3 reports the spectra, in the CN stretching region, of increasing coverages of $CD_3CN$ adsorbed on TS-1 and silicalite-1, top and bottom spectra, respectively. In the inset, the effect on the 960 $cm^{-1}$ band (fingerprint band associated to a skeleton mode involving Ti[21,33,34]) is illustrated. For silicalite-1 we observe the formation, upon $CD_3CN$ dosage,

**Scheme 1**

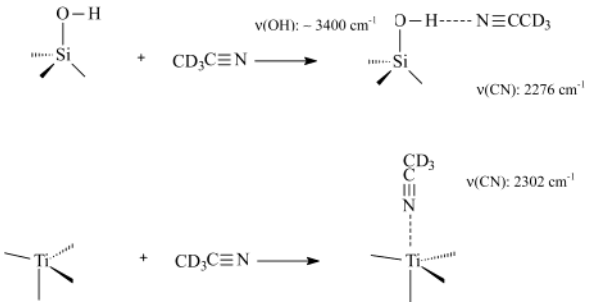


of a single band centered at 2276 $cm^{-1}$ ascribed to the $\bar{\nu}$(CN) of $CD_3CN$ interacting with silanols. Only at highest coverages we observe the growth of a second component at 2265 $cm^{-1}$ associated to physically adsorbed $CD_3CN$. The small blue shift ($\Delta\bar{\nu} = +11$ $cm^{-1}$) of $\bar{\nu}$(CN) mode caused by the interaction with silanols confirms that these species have a very low acidity. In fact, in the presence of strong Brønsted sites ($CD_3CN$/H-ZSM-5 system) $\bar{\nu}$(CN) has been observed at 2298 $cm^{-1}$ ($\Delta\bar{\nu} = +33$ $cm^{-1}$).[35−37]

For TS-1 we observe, starting from very low coverages, the appearance of a totally new component at 2302 $cm^{-1}$ ($\Delta\bar{\nu} = +37$ $cm^{-1}$). This band appears nearly contemporarily to the $\bar{\nu}$(OH···$NCCD_3$) absorption, grows in a parallel way, and does not change its position upon increasing the $CD_3$-CN equilibrium pressure. For sake of comparison, we consider that $CH_3CN$ adsorbed on $TiO_2$ anatase shows a $\Delta\bar{\nu}_{(CN)}$ of +37 $cm^{-1}$, ascribed to the interaction of $CH_3CN$ with less coordinated surface Ti(IV) sites.[28,38] On this basis, we assign the absorption at 2302 $cm^{-1}$ to a direct interaction of CN with Ti(IV) which acts as a medium-strength Lewis site. Finally, we mention that in zeolites containing strong Lewis species, such as uncoordinated $Al_{3c}^{3+}$, a component at 2315 $cm^{-1}$ has been observed.[39]

Only at the $CD_3CN$ equilibrium vapor pressure, the component at 2302 $cm^{-1}$ becomes broader and the position of its maximum shifts to lower wavenumbers (about 2297 $cm^{-1}$) because of solvation effects associated with the filling of the channels, which decrease the effects of the direct Ti(IV)···$NCCD_3$ interaction. All the species are easily and completely reversible (spectra not shown). The fact that the Ti(IV)···$NCCD_3$ band, even if associated with strongly perturbed $CD_3CN$ ($\Delta\bar{\nu} = +37$ $cm^{-1}$), is no more resistant to desorption than that associated with the less perturbed ($CD_3CN$···OH) species ($\Delta\bar{\nu} = +11$ $cm^{-1}$), suggests that the involved complexes have similar stabilities. This apparent contradiction will be discussed in section 4, when ab initio computations will be reported and discussed.

Spectra reported in the inset confirm that $CD_3CN$ interacts directly with Ti(IV) species. Upon $CD_3CN$ dosages, we observe a clear broadening and a blue shift of the 960 $cm^{-1}$ band to 970 $cm^{-1}$. This behavior is a clear indication that the probe molecule is interacting directly with Ti(IV).[10−14,21,33,34] The interaction of $CD_3CN$ with hydroxyls and Ti(IV) is summarized in Scheme 1. It can so be concluded that, unlike $H_2O$ and $NH_3$,[14] $CD_3CN$ is a

(33) Scarano, D.; Zecchina, A.; Bordiga, S.; Geobaldo, F.; Spoto, G.; Petrini, G.; Leofanti, G.; Padovan, M.; Tozzola, G. *J. Chem. Soc., Faraday Trans.* **1993**, *89*, 4123.
(34) Ricchiardi, G.; Damin, A.; Bordiga, S.; Lamberti, C.; Spanò, G.; Rivetti, F.; Zecchina, A. *J. Am. Chem. Soc.* **2001**, *123*, 11409.
(35) Pelmenschikov, A. G.; van Santen, R. A.; Jänchen, J.; Meijer, E. *J. Phys. Chem.* **1993**, *97*, 11071.
(36) Medin, A. S.; Borovkov, V. Yu.; Kazansky, V. B.; Pelmenschikov, A. G.; Zhidomirov, G. M. *Zeolites* **1990**, *10*, 668.
(37) Otero Areán, C.; Escalona Platero, E.; Peñarroya Mentruit, M.; Rodríguez Delgado, M.; Llabrés i Xamena, F. X.; García-Raso, A.; Morterra, C. *Microporous Mater.* **2000**, *34*, 55.
(38) Busca, G.; Saussey, H.; Saur, O.; Lavalley, J. C.; Lorenzelli, V. *Appl. Catal.* **1985**, *14*, 245.
(39) Knözinger, H.; Krietenbrink, H. *J. Chem. Soc., Faraday Trans.* **1975**, *71*, 2421.

**Table 1. Geometric Features of the $Ti(OSi)_4$ Moieties in Optimized Bare MFI_T16 Model (see Figure 1)[a]**

| model | Ti−O/Å | α/° | β/° | Ti−CM/ Å | Ti−O−Si/° | Ti−Si/Å |
|---|---|---|---|---|---|---|
| MFI_T16 | 1.797−1.813 | 110.5−111.3 | 106.4−109.4 | 0.559 | 146.2, 151.3, 168.6, 169.5 | 3.306−3.426 |
| EXAFS | 1.79−1.81 ± 0.01 | | | | (143, 143, 162, 162) ± 5 | 3.26−3.38 ± 0.02 |

[a] Experimental EXAFS data are obtained from refs 43 and 45.

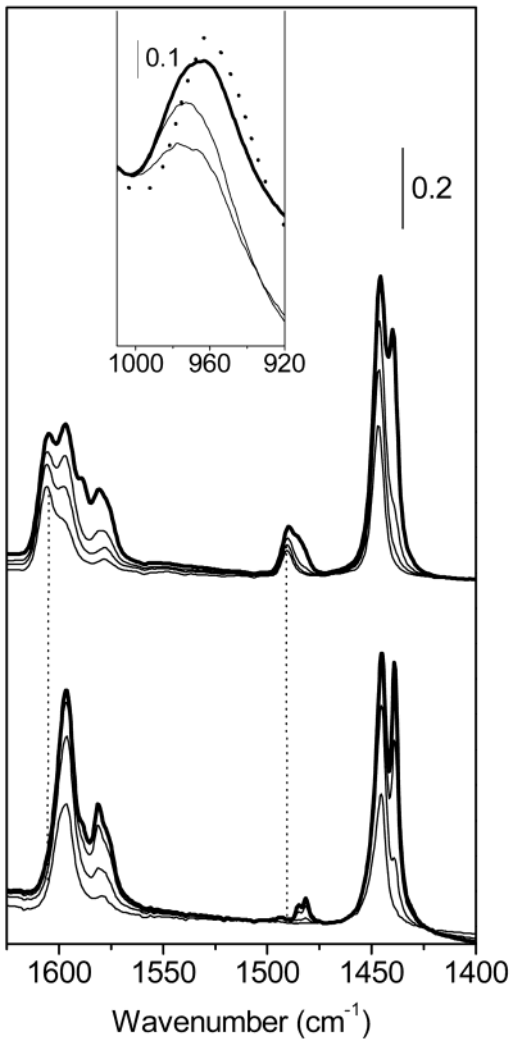


**Figure 4.** Background-subtracted spectra of increasing coverages of pyridine on TS-1 (top) and on silicalite-1 (bottom). The spectra obtained at high pyridine coverage are reported with a bold line. The inset reports the perturbative effect of pyridine on the 960 $cm^{-1}$ band: pure TS-1 spectrum is reported with a dotted line, while the bold line represents the spectrum obtained after 3 h of pumping.

selective IR probe of the Lewis acidity associated with the presence of Ti(IV) in the framework.

**3.3 Ti(IV)/Pyridine Adducts.** Figure 4 shows the IR spectra of pyridine adsorbed on TS-1 (top) and silicalite-1 (bottom) in the 1650−1400 $cm^{-1}$ range of the ring-stretching modes. All spectra are background subtracted and are obtained after contact with saturated pyridine vapor and successive outgassing for increasing time (last spectra have been recorded after 30 min of pumping).

In the spectra obtained on silicalite-1 sample, the ring-stretching modes of hydrogen-bonded (hb) and physically (ph) adsorbed pyridine are clearly observed at 1597 (hb, mode 8a), 1588 (ph, mode 8a), 1581 (hb, ph, mode 8b), 1485 (hb, mode 19a), 1481 (ph, mode 19a), 1444 (hb, mode 19b), and 1439 $cm^{-1}$ (ph, mode 19b).[31] The discrimination between the bands because of physically adsorbed and hydrogen-bonded pyridine is a simple operation which is

**Scheme 2**

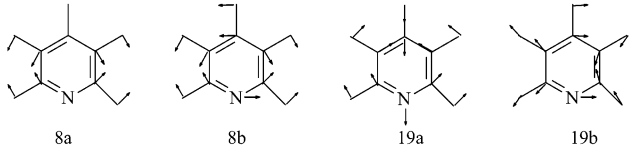


based on the different behavior of the bands upon desorption at RT; the bands associated with hydrogen-bonded pyridine are more resistant. The ring-stretching mode frequencies observed for physically adsorbed pyridine are in accordance with those reported by Kline and Turkevich[30] for pure pyridine: 1580 (8a), 1570 (8b), 1485 (19a), and 1440 $cm^{-1}$ (19b) (see Scheme 2 for normal mode representation).

The top part of Figure 4 reports the spectra obtained upon pyridine adsorption on TS-1. As evidenced by the straight dotted lines, which connect the spectra obtained on TS-1 to those ones obtained on silicalite-1, it is possible to single out the presence of new components. In particular, we observe two new distinct maxima at 1604 and at 1490 $cm^{-1}$ and a shoulder at 1450 $cm^{-1}$, which are absent in the bottom spectra (silicalite-1). All the new components are more resistant to the pumping.

The presence of new components specifically related to the presence of Ti(IV) suggests, once again, a direct interaction between the ligand (pyridine) and Ti(IV) centers. On this basis, the bands at 1604 and 1490 $cm^{-1}$ can be assigned to the modes 8a and 19a, respectively, of pyridine interacting with a weak Lewis acid Ti(IV) center. The perturbation induced on the modes 8b and 19b is definitely smaller. These bands are therefore superimposed to those of hydrogen-bonded species.

As pyridine adsorbed on pure $TiO_2$ shows the mode 8a at 1606 $cm^{-1}$ (see ref 40), we can affirm (as it has already been concluded in the $CD_3CN$ interaction) that the Lewis acidity of Ti(IV) in TS-1 is quite similar to that exhibited by the coordinatively unsaturated Ti(IV) centers of a $TiO_2$ sample. This assignment is supported by comparison with IR experiments of pyridine dosed on $\gamma$-$Al_2O_3$ (a solid characterized by strong Lewis acid sites), where four bands at 1620 (8a), 1578 (8b), 1492 (19a), and 1450 (19b) $cm^{-1}$ are observed.[41,42]

The direct interaction of pyridine with Ti(IV) is also documented by the behavior of the band centered at 960 $cm^{-1}$ (inset of Figure 4) in the presence of adsorbed pyridine. Upon pyridine dosage (full coverage), the original absorption becomes very broad, less intense, and shifted to higher frequency (maximum at 974 $cm^{-1}$). By outgassing for increasing time, a progressive shift to lower frequencies is observed, even if the original band is not fully restored (last spectrum is reported in bold). This behavior is in agreement with previous considerations. The spectroscopic evidences of pyridine interactions are summarized in Scheme 3 (note that the 8b mode exhibits a similar envelope in both TS-1 and silicalite-1 cases, so that no frequency can be safely ascribed to the $C_5H_5N\cdots$Ti(IV) adduct).

(40) Morterra, C.; Cerrato, G.; Visca, M.; Lenti, D. M. *Mater. Chem. Phys.* **1991**, *28*, 151.
(41) Morterra, C.; Magnacca, G. *Catal. Today* **1996**, *27*, 497.
(42) Yamamoto, T.; Tanaka, T.; Matsuyama, T.; Funabiki, T.; Yoshida, S. *J. Phys. Chem.* **2001**, *105*, 1908.

**Table 2. Geometric and Energetic Features of the $Ti(OSi)_4$ Moieties in the MFI_T16 Optimized Cluster upon Adsorption of $CH_3CN$ and $C_5H_5N$ Molecules (L = $CH_3CN$ and $C_5H_5N$, Respectively)[a]**

| L | Ti−O/Å | Δ<Ti−O>/ Å | α/° | β/° | Ti−CM/ Å | Ti−O−Si/° | Ti−Si/ Å | Ti−L/Å | BE/ kJ $mol^{-1}$ | $BE^c$/kJ $mol^{-1}$ |
|---|---|---|---|---|---|---|---|---|---|---|
| $CH_3CN$ | 1.818−1. 828 | +0.016 | 116.8−117.9 | 98.6−100.4 | 0.304 | 151.2, 157.2, 165.4, 177.1 | 3.350−3.447 | 2.46 | +15.0 | +4.8 |
| $C_5H_5N$ | 1.826−1. 842 | +0.025 | 115.3−119.5 | 97.0−99.6 | 0.270 | 150.5, 158.1, 167.3, 176.7 | 3.358−3.451 | 2.39 | +44.2 | +26. 4 |

| L | Δ(C−N)/Å | $\Delta\bar{\nu}$(CN)/$cm^{-1}$ |
|---|---|---|
| $CH_3CN$ | −0.003 | +29 (+37 ) |

| L | Δ(C−N)/Å | Δ(C−C)/Å | $\Delta\bar{\nu}$(19b)/$cm^{-1}$ | $\Delta\bar{\nu}$(19a)/$cm^{-1}$ | $\Delta\bar{\nu}$(8b)/$cm^{-1}$ | $\Delta\bar{\nu}$(8a)/$cm^{-1}$ |
|---|---|---|---|---|---|---|
| $C_5H_5N$ | +0.002/+0.005 | −0.002/−0.005 | +5 (+10) | +5 (+5) | −1 (not available) | +20 (+24) |

[a] For L = $CH_3CN$ the computed variation of C−N distance Δ(C−N) together with computed $\Delta\bar{\nu}$(CN) are listed. For L = $C_5H_5N$ the computed variation of the two C−N distances Δ(C−N) and C−C distances Δ(C−C) together with computed $\Delta\bar{\nu}$ of 19b, 19a, 8b, and 8a modes are reported. For sake of comparison, the experimental $\Delta\bar{\nu}$ for acetonitrile and pyridine are also reported in parentheses.

**Scheme 3**

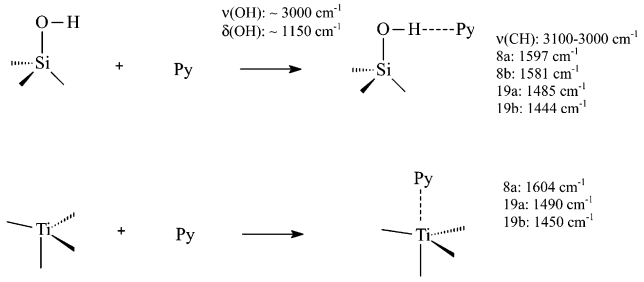


## 4. Computational Results and Discussion

As previously described in Section 2.2, the cluster MFI_T16 (see Figure 1) has been employed to simulate the Ti(IV) site in TS-1 and to study its interaction with acetonitrile and pyridine. Geometrical features of the bare, fully optimized, cluster are listed in Table 1 and are in general good agreement with the experimental data from EXAFS analysis in terms of Ti−O and Ti−Si first and second shells distances and Ti−O−Si angles[43−45] (see section D of ref 19 for a more detailed comparison).

Acetonitrile and pyridine interact with Ti(IV) centers via N atoms, as shown in Figure 5, where the optimized $CH_3CN$/MFI_T16 and $C_5H_5N$/MFI_T16 complexes are reported. The insertion of a ligand molecule causes a Ti−O bond elongation of 0.016 and 0.025 Å, while the calculated Ti···N distances are 2.46 and 2.39 Å for acetonitrile and pyridine, respectively, see Table 2. The same table also reports the variations of some geometrical features of adsorbed molecules with respect to the bare ones, together with calculated $\Delta\bar{\nu}$. As can be seen from Table 2, the interaction with acetonitrile or pyridine causes a further distortion of the $TiO_4$ moiety from the tethraedrical symmetry as monitored by the decrease of the Ti−CM distance and the increase of the α/β splitting: 117°/99° and 118°/98° for acetonitrile and pyridine, respectively (values wich are now close to 120°/90°, characteristic of a bipyramidal geometry). Similar results were already obtained for the interaction of MFI_T16 cluster with $NH_3$ and $H_2O$.[14,19,21] The major distortion obtained for pyridine with respect to the acetonitrile suggests a stronger interaction. This is confirmed by the calculation of $BE^c$ (see Table 2), which is larger for pyridine than for acetonitrile by +21.6 kJ $mol^{-1}$.

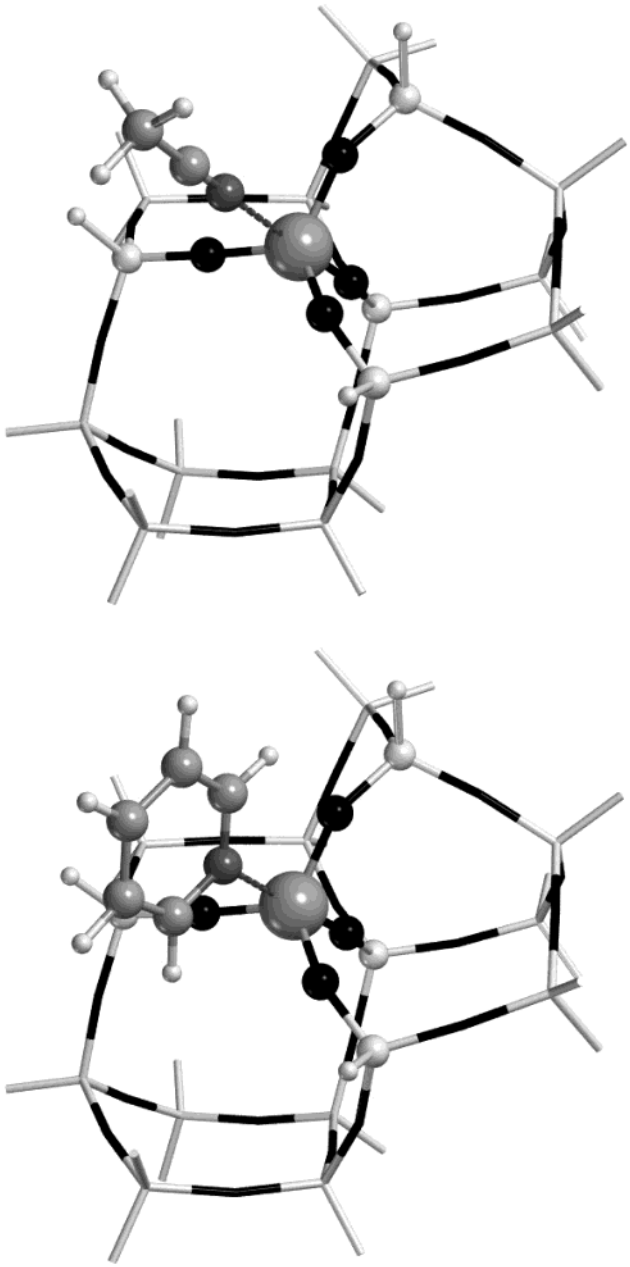

**Figure 5.** Optimized MFI_T16/$CH_3CN$ and MFI_T16/$C_5H_5N$ complexes. The representation style is the same as in Figure 1.

(43) Bordiga, S.; Coluccia, S.; Lamberti, C.; Marchese, L.; Zecchina, A.; Boscherini, F.; Buffa, F.; Genoni, F.; Leofanti, G.; Petrini, G.; Vlaic, G. *J. Phys. Chem.* **1994**, *98*, 4125.

(44) Bordiga, S.; Boscherini, F.; Coluccia, S.; Genoni, F.; Lamberti, C.; Leofanti, G.; Marchese, L.; Petrini, G.; Vlaic, G.; Zecchina, A. *Catal. Lett.* **1994**, *26*, 195.

(45) Gleeson, D.; Sankar, G.; Catlow, C. R. A.; Thomas, J. M.; Spanó, G.; Bordiga, S.; Zecchina, A.; Lamberti, C. *Phys. Chem. Chem. Phys.* **2000**, *2*, 4812.

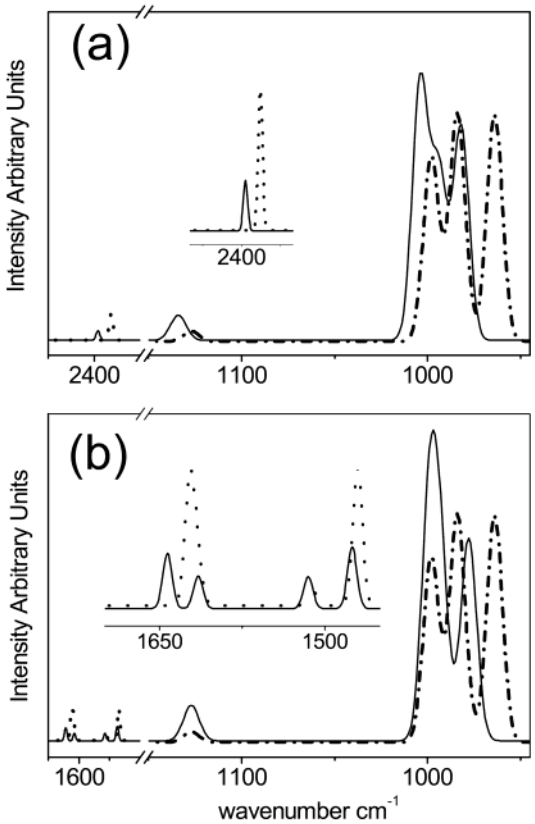


**Figure 6.** Computed IR spectra for the bare MFI_T16 cluster (dot−dashed line), the isolated molecules (dashed lines), and the engaged clusters (full lines). Parts a and b refer to $CH_3CN$ and $C_5H_5N$, respectively.

Figure 6 reports the computed IR spectra for the bare MFI_T16 cluster (dot−dashed line), the isolated molecules (dashed lines), and the engaged $CH_3CN$/MFI_T16 and $C_5H_5N$/MFI_T16 clusters (full lines). Concerning the perturbation of the IR features of the adsorbed molecules (Table 2), the calculations for acetonitrile and pyridine complexes show a qualitative agreement with the experimental results. In particular, in acetonitrile the computed blue-shift (accompanied by a reduction of −0.003 Å of the C−N distance in the adsorbed molecule with respect to the bare one) is slightly underestimated with respect to the experimental one (+29 vs +37 $cm^{-1}$). This suggests a lack of interaction (confirmed also by the extremely low calculated BE[c]) which could be ascribed to the cluster approach here adopted, which underestimates the long-range interaction typical for a crystalline material such as TS-1. In pyridine, the agreement between measured and computed shifts of the molecular modes is even better: 19b (+5 vs +10 $cm^{-1}$), 19a (+5 vs +5 $cm^{-1}$), and 8a (+20 vs +24 $cm^{-1}$), while no comparison is available for the 8b mode (vide supra Scheme 3 and related discussion). Also in this case, the shifts are slightly underestimated. Finally, the interaction of acetonitrile or pyridine with the Ti(IV) center causes a perturbation of the 960 $cm^{-1}$ centered band: the computed spectra for the isolated center are shown in Figure 6. The computed blue-shifts, listed in Table 3, are in qualitative agreement with the experimental ones. See refs 14 and 21 for the definition of modes A and B.

**Table 3. Vibrational Features (*A* and *B* Modes) of Bare and Engaged MFI_T16 Model for TS-1[a]**

| model | $B\bar{\nu}_1$ ($cm^{-1}$) | $B\bar{\nu}_2$ ($cm^{-1}$) | $B\bar{\nu}_3$ ($cm^{-1}$) | $B\langle\bar{\nu}\rangle$ ($cm^{-1}$) | $A$ ($cm^{-1}$) |
|---|---|---|---|---|---|
| MFI_T16 | 964 | 984 | 998 | 980.9 | 1127 |
| MFI_T16/$CH_3CN$ | 982 | 994 | 1004 | 994.0 | 1134 |
| MFI_T16/$C_5H_5N$ | 978 | 993 | 999 | 990.3 | 1127 |

[a] $\langle\bar{\nu}\rangle$ represents the center of mass of the *B* triplet.

## 5. Conclusions

We have reported a combined IR and computational study of the interaction of $CD_3CN$ and pyridine with Ti(IV) centers in TS-1. Because of the ability of both molecules to distinguish between Lewis and Brønsted sites, we were able to single out the vibrational modes of $CD_3CN$ and $C_5H_5N$ molecules adsorbed on Ti(IV) from those adsorbed on the abundant hydroxyl groups. In both cases, we found spectroscopic features which are characteristic of TS-1 and are completely absent in a pure siliceous silicalite-1 matrix. This attempt failed with $H_2O$ and $NH_3$ probes.[14] To the best of our knowledge, this represents the first direct observation of the perturbation of the molecular modes of a probe adsorbed on the Ti(IV) centers of a titanosilicate molecular sieve, which has shown that Ti(IV) centers embedded in the MFI framework have a Lewis acidity strength comparable to that of Ti(IV) sites at the surface of $TiO_2$. These results have also been obtained exploiting the fact that the relevant modes of both $CD_3CN$ and $C_5H_5N$ molecules occur in spectral regions where the matrix (MFI framework with silanol cavities) does not exhibit peculiar absorptions.

These IR data could be of interest also for the quantum chemistry community as useful numbers for testing models describing Ti(IV) sites in titanosilicates. In this work, we also report the first attempt to model the $CD_3CN\cdots$Ti(IV) and $C_5H_5N\cdots$Ti(IV) interaction by means of a cluster approach in the ONIOM scheme.

LA0262194